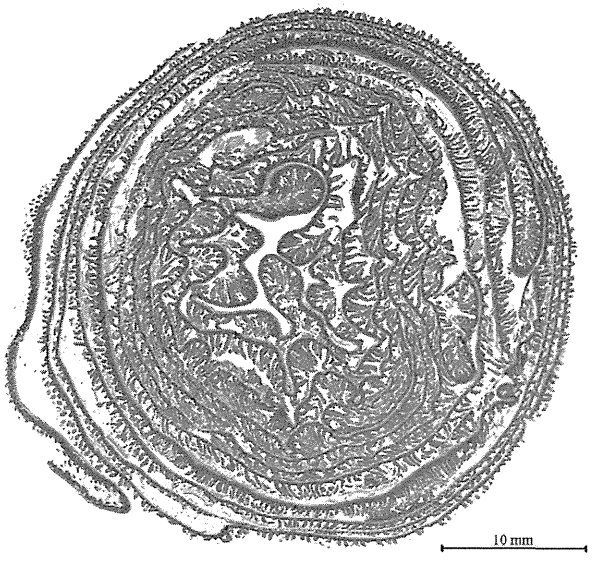

Fig. 1. The 'Swiss roll' technique makes it possible to scan the entire intestinal tract, including the small and large intestines, in a single section. HE. Bar, 10 mm.

method (Yanai *et al.*, 1998), with ABC kits (Vector Laboratories, Burlingame, California, USA). The secondary antibody was biotinylated anti-rabbit IgG (DAKO Cytomation, Carpinteria, California, USA) and liquid DAB substrate chromogen system (DAKO) was used as the chromogen. Sections were counterstained with haematoxylin. Tissue sections from the EHV-9-infected hamsters and sera from a non-immunized rabbit and goat were used as controls.

DNA Extraction and PCR

DNA was extracted from spinal cord, brain and blood using the Sepagene kit for virus DNA detection (Sanko pharmacological Co., Tokyo, Japan). Viral DNA was detected using primers for the open reading frame (ORF)76-F (5′TTT CCC TCT CAG CGA TCA CTT TTC ACC ACC GAA GAA CAG GCC CTC ATC GG 3′) and ORF76-R (5′ GGG CTG TTG TGG GGT AAA AGG TGG TGT TAC GGA AAC ACG CGT GCC AAG AA 3′). PCR amplification was performed in 50 µl volumes containing DNA (100 ng), 8 µl of each dNTP, 0.5 µl of each primer, 25 µl LA Taq Buffer (Mg^{+2} plus) and 0.5 µl Takara LA *Taq*™ DNA polymerase (Takara, Kyoto, Japan). The PCR conditions were as follows: 5 min at 94°C (initial denaturation), 30 cycles of 5 sec at 98°C, 30 sec at 68°C and 90 sec at 72°C, and finally 7 min at 72°C (final extension). The PCR product was separated in an agarose gel (0.9%) and stained with ethidium bromide.

Results

ICR Mice

ICR mice inoculated with EHV-9 showed no apparent clinical signs, except for a minimal loss of body weight. No gross abnormalities were observed in the viscera or central nervous system (CNS) at the time of necropsy examination.

Histopathological findings are summarized in Table 1. In mice killed at 36 hpi there was moderate hyperkeratosis of the stratified squamous epithelium of the forestomach (Fig. 2a). At 48–72 hpi there was moderate to severe gastritis with erosion or ulceration and multifocal neutrophilic infiltration of the submucosa, with dilation of submucosal blood vessels (Fig. 2b).

At 48 hpi the mice inoculated with EHV-9 had moderate interstitial pneumonia characterized by diffusely thickened alveolar septa with varying degrees of macrophage and neutrophil infiltration. There were multifocal areas of hepatocyte degeneration after 72 hpi.

The severity and distribution of CNS lesions are summarized in Table 2. There was meningoencephalitis at the level of the pons, characterized by moderate neuronal degeneration, gliosis and perivascular aggregation of lymphocytes, plasma cells and neutrophils, with mild meningeal lymphocytic infiltration at 72 hpi. At 96 hpi the lesions extended to the medulla oblongata and the cerebellum and hippocampus were moderately affected. At 120 hpi the moderate neuronal loss and gliosis extended to the olfactory bulb, especially affecting the granular cell layer, and there were frequent intranuclear inclusions in the neurons of the pons and medulla oblongata. By 144 hpi, meningoencephalitis had extended to involve most of the brain, including all layers of the olfactory bulb except the glomerular layer.

Table 3 shows the time–course distribution of EHV-9 antigen in the internal organs. At 12 hpi, EHV-9 antigen was seen in macrophages within the lingual muscles (Fig. 3). In addition, at 48 hpi virus antigen was detected in the stratified squamous epithelium of the forestomach and in inflammatory cells in the underlying submucosa.

Virus antigen was frequently detected in the bronchial and alveolar epithelium and alveolar macrophages at 48 hpi. At 72 hpi there was occasional labelling of the nuclei and cytoplasm of hepatocytes and at 120 hpi this labelling was more widespread and associated with the formation of inclusion bodies (Fig. 4). There was no EHV-9 antigen in the myenteric plexuses of the gastrointestinal tract.

The time–course distribution of EHV-9 antigen in the CNS in mice inoculated orally with EHV-9 is

Table 1
Time–course distribution and severity of microscopical lesions in organs of animals inoculated orally with EHV-9

Animal	*ICR mice*								*Suckling Syrian hamsters*					
	Hours post inoculation								*Hours post inoculation*					
	12	*24*	*36*	*48*	*72*	*96*	*120*	*144*	*12*	*24*	*36*	*48*	*72*	*96*
Oral cavity														
Mucosa	ND	ND	ND	ND	ND	ND	ND	ND	–	–	–	–	–	–
Submucosa	ND	ND	ND	ND	ND	ND	ND	ND	+	++	+++	+++	+++	++
Tongue	+	++	+++	+++	++	++	+	+	+	+	+	++	++	+
Forestomach														
Mucosa	–	–	+	++	+++	+	+	–	–	–	+	+	++	++
Submucosa	–	–	+	+	++	++	+	–	–	–	–	+	+	++
Myenteric plexuses	–	–	–	–	–	–	–	–	–	–	–	–	+	+
Glandular stomach														
Mucosa	–	–	–	–	–	–	–	–	–	–	–	–	–	–
Submucosa	–	–	–	–	–	–	–	–	–	–	–	–	+	+
Myenteric plexuses	–	–	–	–	–	–	–	–	–	–	–	–	–	–
Small intestine														
Mucosa	–	–	–	–	–	–	–	–	–	–	–	+	++	+++
Submucosa	–	–	–	–	–	–	–	–	–	–	–	+	+	++
Myenteric plexuses	–	–	–	–	–	–	–	–	–	–	–	–	+	+
Large intestine														
Mucosa	–	–	–	–	–	–	–	–	–	–	–	+	+	+++
Submucosa	–	–	–	–	–	–	–	–	–	–	–	–	+	++
Myenteric plexuses	–	–	–	–	–	–	–	–	–	–	–	–	+	+
Liver	–	–	–	–	+	+	++	++	–	–	–	+	++	+++
Lung														
Bronchi and bronchioles	–	–	–	+	+	++	++	+++	–	–	+	++	+++	+++
Alveoli	–	–	–	–	+	+	++	+++	–	–	+	+	++	+++
Heart	–	–	–	–	–	–	–	–	–	–	–	–	–	+

Severity score: –, none; +, slight; ++, moderate; +++, severe. ND, not detected.

shown in Table 4. After inoculation, EHV-9 antigen was first observed in the meninges and pons at 72 hpi, followed by the medulla oblongata and cerebellum at 96 hpi. EHV-9 antigen was observed in the granular layer of the olfactory bulb at 120 hpi. By 144 hpi, EHV-9 antigen was seen throughout the brain, including the midbrain, hippocampus and all layers of the olfactory bulb except the glomerular layer.

Suckling Hamsters

Most of the inoculated suckling hamsters showed neurological signs in the form of depression and

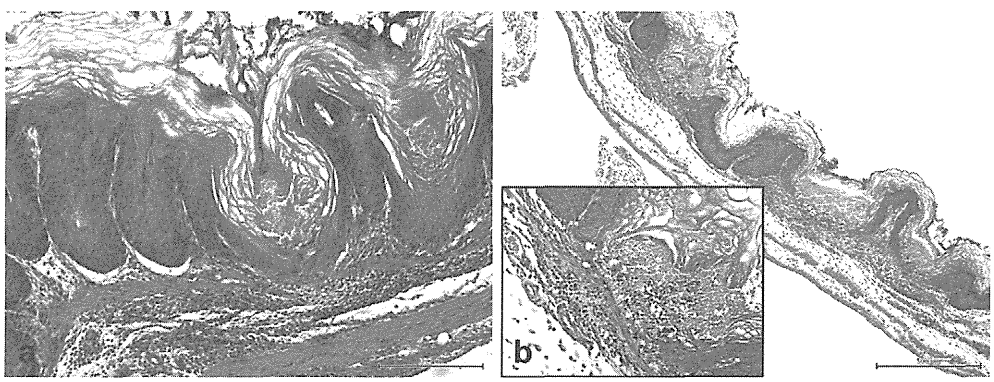

Fig. 2. (a) Forestomach of an ICR mouse at 36 hpi showing moderate hyperkeratosis with submucosal inflammation. HE. Bar, 200 μm. (b) Forestomach of an ICR mouse at 72 hpi showing multifocal ulceration and diffuse lymphocytic infiltration. HE. Bar, 500 μm (Inset, 100 μm).

Table 2
Time–course distribution and severity of microscopical lesions in the CNS of animals inoculated orally with EHV-9

Animal	*ICR mice*								*Suckling Syrian hamsters*					
	Hours post inoculation								*Hours post inoculation*					
	12	*24*	*36*	*48*	*72*	*96*	*120*	*144*	*12*	*24*	*36*	*48*	*72*	*96*
Trigeminal ganglia and nerve	ND	ND	ND	ND	ND	ND	ND	ND	–	–	+	+ +	+ + +	+ + +
Brain														
Cerebrum														
Olfactory bulb														
Glomerular layer	–	–	–	–	–	–	–	–	–	–	–	–	+	+ +
Mitral layer	–	–	–	–	–	–	–	+	–	–	–	–	+	+ +
Granular layer	–	–	–	–	–	–	+	+ +	–	–	–	–	–	+
Thalamus	–	–	–	–	–	–	+	+ +	–	–	–	–	+	+ +
Hippocampus	–	–	–	–	–	+	+ +	+ +	–	–	–	–	+	+ +
Midbrain	–	–	–	–	–	+	+ +	+ +	–	–	–	+	+	+
Cerebellum	–	–	–	–	–	+	+ +	+ +	–	–	–	–	+	+ +
Brainstem														
Pons	–	–	–	–	+	+ +	+ +	+ + +	–	–	–	+	+ +	+ + +
Medulla oblongata	–	–	–	–	–	+	+ +	+ +	–	–	–	–	+	+ +
Meninges	–	–	–	–	+	+	+ +	+ +	–	–	–	+	+ +	+ + +
Spinal cord														
Cervical portion	–	–	–	–	–	–	–	–	–	–	–	–	–	+
Dorsal root ganglia	–	–	–	–	–	–	–	–	–	–	–	–	–	–
Meninges	–	–	–	–	–	–	–	–	–	–	–	–	–	+

Severity score: –, none; +, slight; + +, moderate; + + +, severe. ND, not determined.

Table 3
Time–course distribution of EHV-9 antigen in the organs of animals inoculated orally with EHV-9

Animal	*ICR mice*								*Suckling Syrian hamsters*					
	Hours post inoculation								*Hours post inoculation*					
	12	*24*	*36*	*48*	*72*	*96*	*120*	*144*	*12*	*24*	*36*	*48*	*72*	*96*
Oral cavity														
Mucosa	ND	ND	ND	ND	ND	ND	ND	ND	–	–	–	–	–	–
Submucosa	ND	ND	ND	ND	ND	ND	ND	ND	+	+ +	+ +	+	+	–
Tongue	+	+	+	+	+	+	+	–	+	+	+ +	+	+	–
Forestomach														
Mucosa	–	–	–	+	+	+ +	+	–	–	–	+	+ +	+ +	+ +
Submucosa	–	–	–	+	+ +	+ +	+	–	–	–	+	+ +	+ +	+
Myenteric plexuses	–	–	–	–	–	–	–	–	–	–	–	–	+	+ +
Glandular stomach														
Mucosa	–	–	–	–	–	–	–	–	–	–	–	–	–	–
Submucosa	–	–	–	–	–	–	–	–	–	–	–	–	–	–
Myenteric plexuses	–	–	–	–	–	–	–	–	–	–	–	–	–	+
Small intestine														
Mucosa	–	–	–	–	–	–	–	–	–	–	–	+	+ +	+ + +
Submucosa	–	–	–	–	–	–	–	–	–	–	–	–	+	+ +
Myenteric plexuses	–	–	–	–	–	–	–	–	–	–	–	–	–	+
Large intestine														
Mucosa	–	–	–	–	–	–	–	–	–	–	–	+	+ +	+ + +
Submucosa	–	–	–	–	–	–	–	–	–	–	–	+	+	+ +
Myenteric plexuses	–	–	–	–	–	–	–	–	–	–	–	–	–	+
Liver	–	–	–	–	+	+ +	+ +	+ + +	–	–	–	+	+ +	+ + +
Lung														
Bronchi and bronchioles	–	–	–	+	+	+ +	+ +	+ + +	–	–	–	+	+ +	+ + +
Alveoli	–	–	–	–	+	+	+ +	+ + +	–	–	–	+	+ +	+ +
Heart	–	–	–	–	–	–	–	–	–	–	–	–	–	+

Presence of viral antigen: –, negative; +, occasional; + +, moderate; + + +, frequent. ND, not determined.

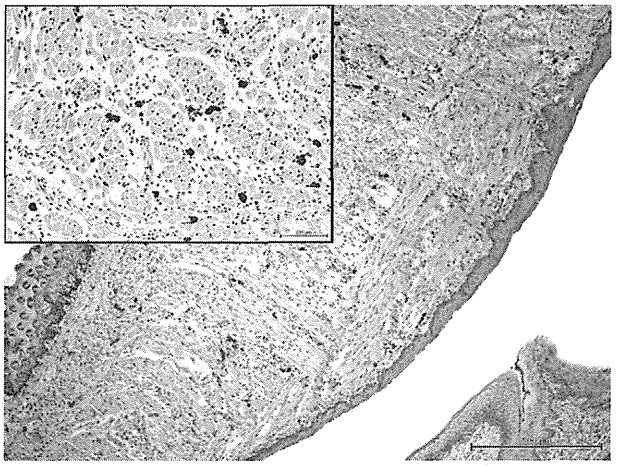

Fig. 3. Expression of EHV-9 antigen within macrophages in the tongue of an ICR mouse at 24 hpi. IHC. Bar, 500 μm (Inset, 200 μm).

uncoordinated movement at 72 hpi and thereafter, and the clinical signs continued until the end of the experiment at 96 hpi. All of the animals died during this hour so the planned schedule was not completed.

No gross abnormalities were detected in the internal organs of the hamsters inoculated orally with EHV-9.

The time–course distribution of microscopical lesions in the viscera is shown in Table 1. After inoculation (12 hpi) there was a slight inflammatory reaction, consisting mainly of macrophages, in the submucosa of the oral cavity and tongue, after which continuous moderate or severe inflammation was observed in the oral cavity. Starting from 36 hpi, slight to moderate inflammatory reactions, mainly lymphocyte and macrophage infiltrations, were observed in the submucosa of the forestomach, and the myenteric plexuses had slight degeneration at 72 and 96 hpi.

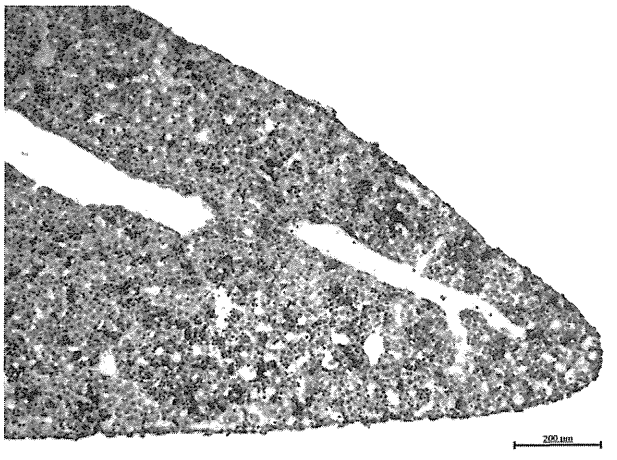

Fig. 4. Expression of EHV-9 antigen in the nucleus and cytoplasm of hepatocytes in an ICR mouse at 120 hpi. IHC. Bar, 200 μm.

There were no significant lesions related to inoculation in the glandular stomach, except for moderate inflammation of the submucosa. In the small and large intestines, slight to moderate degenerative changes in the mucosal epithelium were observed after 48 hpi and slight degenerative changes and inflammatory reactions were seen in the myenteric plexuses at 72 hpi. At 96 hpi there was severe necrotic enteritis characterized by varying degrees of superficial necrosis of the villi with desquamation of the epithelium, and hyperaemia, haemorrhage, oedema and fibrinous exudation in the lamina propria, as well as lymphocytic inflammatory infiltration of the small and large intestines. In severely affected animals there was an associated peritonitis (Fig. 5a).

From 36 hpi there was slight to severe interstitial pneumonia characterized by extensive infiltration with inflammatory cells and thickened alveolar septa (Fig. 6a). In the liver there were mild to severe focal degenerative changes or necrosis of hepatocytes from 48 hpi, and frequent intranuclear inclusions appeared in the lesions in severely affected animals from 96 hpi.

Table 2 shows the time–course distribution and severity of microscopical lesions in the CNS. No abnormalities were detected in the CNS between 12 and 24 hpi. At 36 hpi, mild degeneration and vacuolation were observed in the nerve bundles of the trigeminal nerve, as well as in the pseudounipolar neurons of the trigeminal ganglia. These changes became more severe and were accompanied by inflammatory infiltration of lymphocytes into the trigeminal nerve and aggregation of lymphocytes in the ganglia by 48 hpi (Fig. 7a). At the same time (48 hpi), most of the affected hamsters exhibited mild lymphocytic meningoencephalitis characterized by various degrees of neuronal degeneration and necrosis, gliosis and perivascular aggregation of lymphocytes, plasma cells and neutrophils, starting around the root of the trigeminal nerve entrance at the level of the brainstem (Fig. 8a). There were also mild focal lymphocytic infiltrates in the meninges. In the spinal cord, at 96 hpi there was severe chromatolysis and/or karyorrhexis in degenerating neuronal cells. These cells (mainly in the cervical spinal cord) had frequent intranuclear inclusion bodies. In the grey matter of the spinal cord there was frequent necrosis of neurons, as well as gliosis and perivascular lymphocyte aggregation at 96 hpi (Fig. 9a).

Table 3 shows the time–course detection of EHV-9 antigen in hamsters inoculated with EHV-9. At 12 hpi there was intense labelling of EHV-9 antigen in migrating macrophages in the oral and lingual submucosa. Subsequently, more intense and frequent

Table 4
Time–course distribution of EHV-9 antigen in the CNS of animals inoculated orally with EHV-9

Animal	*ICR mice*								*Suckling Syrian hamsters*					
	Hours post inoculation								*Hours post inoculation*					
	12	*24*	*36*	*48*	*72*	*96*	*120*	*144*	*12*	*24*	*36*	*48*	*72*	*96*
Trigeminal ganglia and nerve	ND	ND	ND	ND	ND	ND	ND	ND	–	–	+	+ +	+ +	+
Brain														
Cerebrum														
Olfactory bulb														
Glomerular layer	–	–	–	–	–	–	–	–	–	–	–	–	+	+ +
Mitral layer	–	–	–	–	–	–	–	+	–	–	–	–	+	+ +
Granular layer	–	–	–	–	–	–	+	+ +	–	–	–	–	–	+
Thalamus	–	–	–	–	–	–	+	+ +	–	–	–	–	+	+ +
Hippocampus	–	–	–	–	–	+	+ +	+ +	–	–	–	–	+	+ +
Midbrain	–	–	–	–	–	+	+ +	+ +	–	–	–	+	+ +	+ + +
Cerebellum	–	–	–	–	–	+	+ +	+ +	–	–	–	–	+	+
Brainstem														
Pons	–	–	–	–	+	+ +	+ + +	+ + +	–	–	–	+	+ +	+ + +
Medulla oblongata	–	–	–	–	–	+	+ +	+ + +	–	–	–	–	+	+ +
Meninges	–	–	–	–	+	+ +	+ +	+ +	–	–	+	+ +	+ +	+
Spinal cord														
Cervical portion	–	–	–	–	–	–	–	–	–	–	–	–	–	+
Dorsal root ganglia	–	–	–	–	–	–	–	–	–	–	–	–	–	–
Meninges	–	–	–	–	–	–	–	–	–	–	–	–	+	+ +

Presence of viral antigen: –, negative; +, occasional; + +, moderate; + + +, frequent. ND, not determined.

positive reactions were seen in macrophages in the oral cavity and tongue at 24 hpi; some of these cells were aggregating around nerve endings in this area (Fig. 10). In the forestomach, EHV-9 antigen was first detected in the stratified squamous epithelium at 36 hpi and thereafter was observed in the submucosa. The glandular stomach had no positive labelling, but the myenteric plexuses in this location expressed EHV-9 antigen later in the experiment. In the small and large intestines there was positive labelling of EHV-9 in the mucosa, especially in the small intestine, starting at 48 hpi and becoming more prominent afterwards (Fig. 5b). Intestinal myenteric plexuses expressed EHV-9 antigen at 96 hpi (Fig. 5c).

In the lungs, EHV-9 antigen was frequently observed in the bronchial and alveolar epithelium as well as the alveolar macrophages at 48 hpi and thereafter (Fig. 6b). In the liver, EHV-9 antigen was first observed in the hepatocytes at 72 hpi and thereafter, and continued to be present until the end of the experiment. Positive reactions were also observed in and around intranuclear inclusions in the hepatocytes at 96 hpi. In the heart, at 96 hpi there were frequent focal areas of labelling in the myocardium and these were observed less frequently in the pericardium (Fig. 11).

In the CNS (Table 4), EHV-9 antigen was detected in the nerve fibres of the trigeminal nerve (Fig. 7b) at 36 hpi and at 48 hpi in the nuclei and

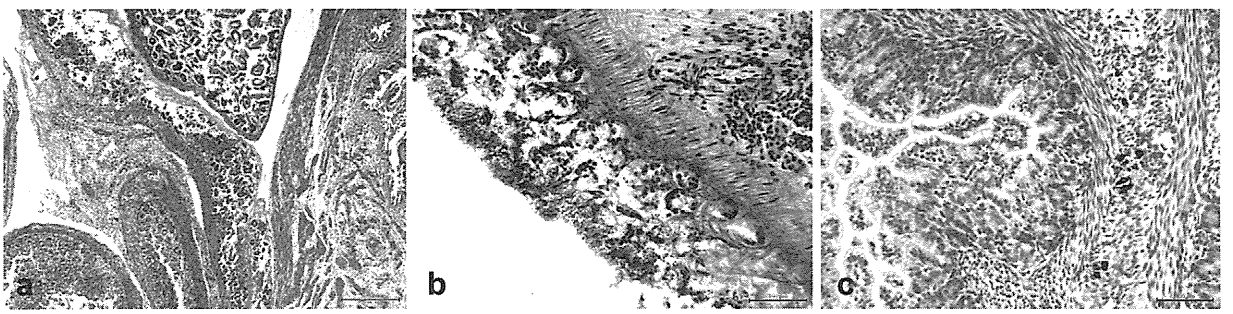

Fig. 5. (a) Necrosis of most villi and serosal adhesions of the small intestine of a suckling hamster at 96 hpi. HE. Bar, 500 µm. (b) Expression of EHV-9 antigen in the mucosal layer of the small intestine of a suckling hamster at 96 hpi. IHC. Bar, 100 µm. (c) Expression of EHV-9 antigen in the neurons of the myenteric plexus of a suckling hamster at 96 hpi. IHC. Bar, 100 µm.

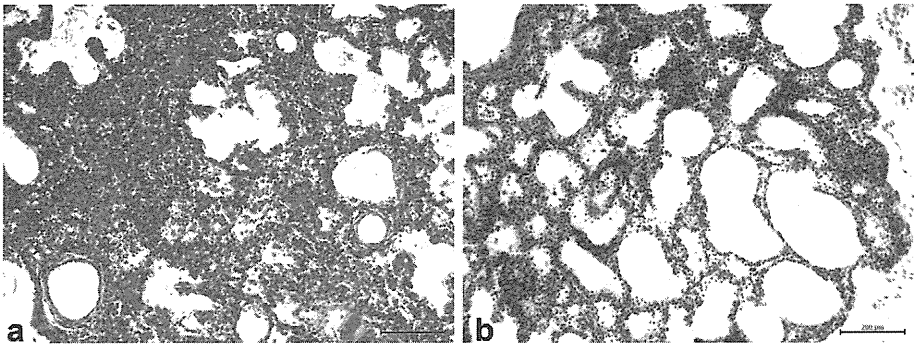

Fig. 6. (a) Interstitial pneumonia characterized by diffusely thickened alveolar septa with macrophage and neutrophil infiltration of the lung of a suckling hamster at 48 hpi. HE. Bar, 200 μm. (b) Expression of EHV-9 antigen in the bronchial and alveolar epithelium and macrophages in the lung of a suckling hamster at 48 hpi. IHC. Bar, 200 μm.

cytoplasm of pseudounipolar neurons of the trigeminal ganglia, the meninges and the brainstem (especially the pons and the root of the trigeminal nerve entrance) (Fig. 8b). EHV-9 antigen was found mainly in the pons at 48 hpi and had extended to involve the cerebellum, medulla oblongata, midbrain and glandular layer of the olfactory bulb by 72 hpi. By 96 hpi, EHV-9 antigen was detected in most parts of the brain, including all layers of the olfactory bulb, as well as in the spinal cord, especially the cervical portion (Fig. 9b). The time–course distribution of detection of EHV-9 antigen in the CNS is shown in Fig. 12a,b and c.

PCR Detection of EHV-9 DNA

EHV-9 DNA was detected in the brain of EHV-9 inoculated hamsters at 36 hpi and thereafter continued to be present until the end of the experiment at 96 hpi. In the spinal cord, EHV-9 DNA was detected only at 96 hpi. In the blood samples, EHV-9 DNA was first detected at 48 hpi and thereafter continued to be present for 3 days.

Discussion

EHV-9 is a newly recognized EHV that was first identified as the cause of fulminant encephalitis in a herd of gazelles in a Japanese zoo (Fukushi *et al.*, 1997). Unlike EHV-1, which is endotheliotropic (Edington *et al.*, 1986), EHV-9 shows strong neurotropism resulting in selective neuronal degeneration and necrosis. Fulminant EHV-9-associated encephalitis with marked neurological signs has now been detected in hamsters, rats, mice, dogs, cats, goats, common marmosets and cattle, raising fears of emerging EHV-9 infection.

A previous experimental study of the infectivity of EHV-9 to rodents by the nasal, oral, ocular, intravenous and intraperitoneal routes revealed that infection by the oral, intraperitoneal and ocular routes was possible, but did not explore the kinetics of the initial stages of infection (El-Habashi *et al.*, 2010b).

The aim of the present study was to clarify the pathogenesis of EHV-9-induced encephalitis after oral inoculation, which is thought to be among the most important routes for virus transmission not only for EHV-9, but also for other neurotropic viruses such

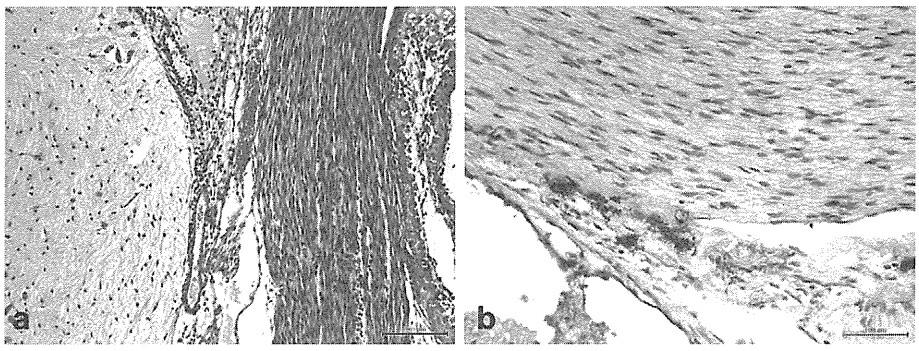

Fig. 7. (a) Neuritis of the trigeminal nerve and mild focal lymphocytic infiltration of the meninges of a suckling hamster at 36 hpi. HE. Bar, 200 μm. (b) Expression of EHV-9 antigen in the trigeminal nerve fibres of a suckling hamster at 36 hpi. IHC. Bar, 100 μm.

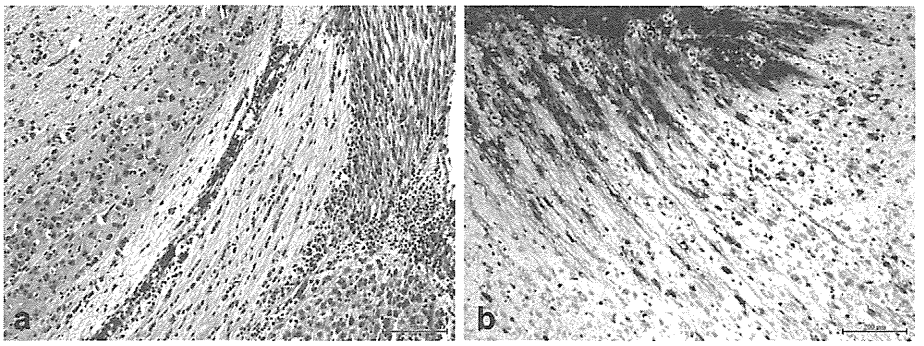

Fig. 8. (a) Neuronal degeneration and necrosis, gliosis and perivascular aggregates of lymphocytes, plasma cells and neutrophils at the root of the trigeminal nerve entrance into the brain of a suckling hamster at 48 hpi. HE. Bar, 200 μm. (b) Expression of EHV-9 antigen at the entrance of the trigeminal nerve to the brain of a suckling hamster at 36 hpi. IHC. Bar, 200 μm.

as pseudorabies virus, Theiler's murine encephalitis virus, bovine herpesvirus type-1 and herpes simplex type-1 (Hagemoser *et al.*, 1980; Ha-Lee *et al.*, 1995; Steiner and Kennedy, 1995). In order to focus on the time–course and distribution of infection, sections of the entire digestive tract, including the oral cavity, tongue, oesophagus, forestomach, glandular stomach and small and large intestines, were examined histologically and immunohistochemically. A Swiss roll technique (Moolenbeek and Ruitenberg, 1981) was used to examine the entire intestinal tract in a single section. In order to examine the potential for the virus to move from the peripheral nerves or ganglia to the CNS, a suckling hamster model was employed (El-Habashi *et al.*, 2010a). Use of these animals made it possible to create sagittal sections that overviewed the nerve connections with the CNS in undecalcified tissue (El-Habashi *et al.*, 2010a). This model was particularly useful for accessing the trigeminal ganglia and nerve with their connection to the brain at the level of the brainstem (pons), as well as connections between the dorsal route ganglia and spinal cord (El-Nahass *et al.*, 2011). By using both techniques, we were able to determine the time–course of infection and demonstrate the primary sites for virus propagation and replication.

In the present study, at 12 hpi EHV-9 viral antigen was detected in macrophages within the oral and lingual submucosa, suggesting a significant role for these cells in viral replication, propagation and transmission. At 24 hpi, a large number of infected macrophages had aggregated and invaded some nerve fibres related to the mandibular and maxillary branches of the trigeminal nerve, thus confirming the role of these structures in transmission of EHV-9 to nervous tissue and in facilitating virus transmission to the CNS. Macrophages may act as a trigger for the mechanism of virus propagation, transmission and spreading from macrophages to target cells, or may

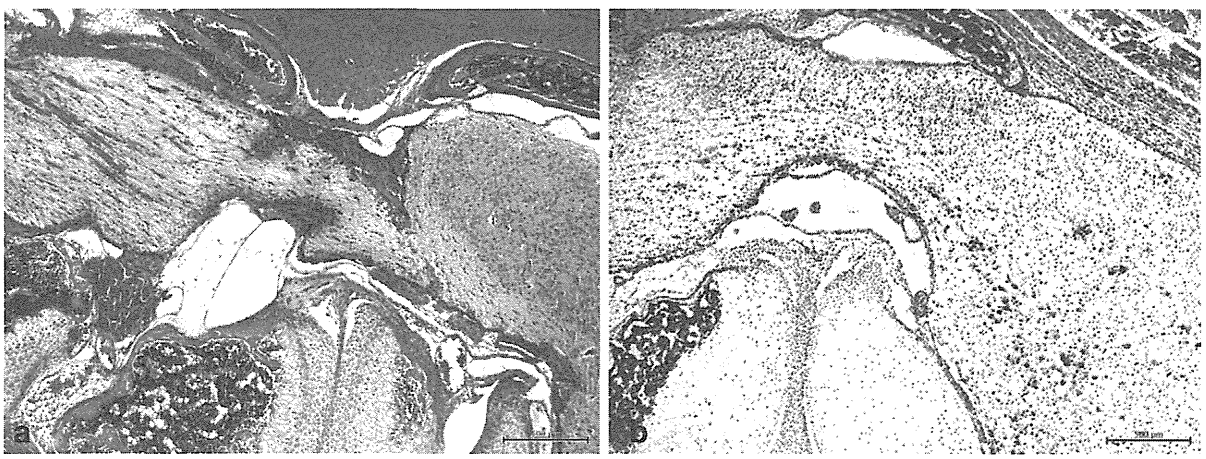

Fig. 9. (a) Meningomyelitis consisting of neuronal necrosis in the grey matter, gliosis and perivascular lymphocytic aggregation in the cervical spinal cord of a suckling hamster at 96 hpi. HE. Bar, 500 μm. (b) Expression of EHV-9 antigen in the cervical spinal cord of a suckling hamster at 36 hpi. IHC. Bar, 500 μm.

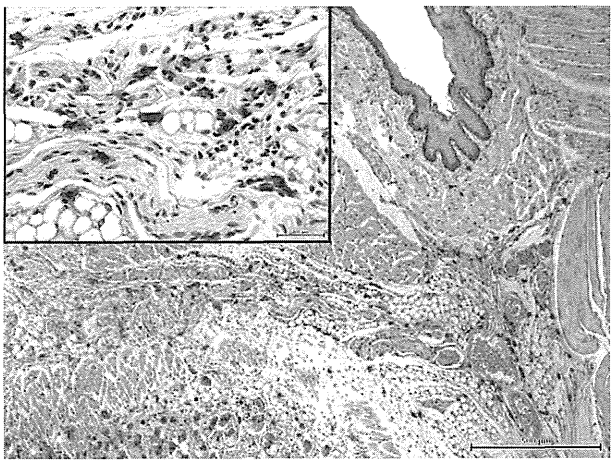

Fig. 10. Expression of EHV-9 antigen in macrophages in the submucosa of the oral cavity in a suckling hamster at 24 hpi. IHC. Bar, 500 μm (Inset, 100 μm).

serve as reservoirs for long-term infection (Bonina *et al.*, 1983; Wu, 2008; Waki and Freed, 2010). In the invasion of simian immunodeficiency virus (SIV) to the CNS, SIV-infected monocytes/macrophages are thought to play an essential role in virus trafficking. This phenomenon underlies the so-called 'Trojan horse theory' of neuroinvasion (Sasseville and Lackner, 1997). A similar mechanism may be involved in CNS infection with equine infectious anemia virus, maedi-visna virus, bovine immunodeficiency virus, caprine arthritis-encephalitis virus, feline immunodeficiency virus and human immunodeficiency virus (Zink *et al.*, 2006). Other reports have suggested that macrophages and freshly recruited monocytes were responsible for the early capture of measles virus (MV), especially in acute infection (Roscic-Mrkic

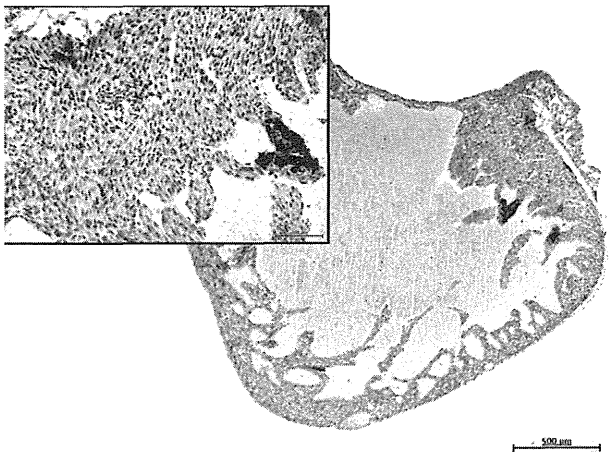

Fig. 11. Expression of EHV-9 antigen in the myocardium of a suckling hamster at 96 hpi. IHC. Bar, 500 μm (Inset, 100 μm).

et al., 2001). The significant role of macrophages has been reported not only after oral inoculation, but also following other routes of inoculation with some neurotropic viruses such as herpes simplex virus type-1, which was trapped by peritoneal macrophages and replicated in these cells following intraperitoneal inoculation of C3H/HeN mice (Bonina *et al.*, 1983) and EHV-9 following intraperitoneal inoculation (El-Nahass *et al.*, 2011).

Based on the results of the present study, it could be postulated that EHV-9 is transmitted mainly by the neuronal pathway, as indicated at 36 hpi by the development of multifocal trigeminal ganglionitis of varying degrees characterized by mononuclear cell infiltration, neuronophagia and neuronal loss in both the trigeminal ganglia and the root of the trigeminal nerve entrance into the brain. Furthermore, the detection of EHV-9 DNA in the brain of suckling hamsters at 36 hpi and from blood samples at 48 hpi was suggestive of a neuronal pathway in virus transmission, primarily via the trigeminal nerve, which is the largest cranial nerve and serves as the largest sensory nerve of the head and face, and the motor nerve of masticatory muscles.

Other reports support this model and show the neuronal transmission of some neurotropic viruses through the trigeminal nerve and ganglia to reach the CNS. This route of infection occurs with SIV, EHV-1, pseudorabies virus and herpes simplex virus. In SIV infection, the virus induces alterations in macaque trigeminal ganglia prior to the occurrence of encephalitis (Aleman *et al.*, 2001; Laast *et al.*, 2007; Pusterla *et al.*, 2010). In Aujeszky's disease virus (ADV) infection of pigs the virus disseminates through the maxillary nerve and trigeminal ganglia and can be isolated after 21 hpi from the trigeminal ganglia (Kritas *et al.*, 1995). Some herpesviruses have natural neurotropism to the trigeminal ganglia, as in the case of EHV-1 and -4 (Borchers *et al.*, 1997).

Another goal of this study was to detect and examine the pathological effects of EHV-9 in internal organs other than the CNS. After oral inoculation with EHV-9, focal erosive or ulcerative gastritis was induced in the forestomach of ICR mice without intestinal involvement, and more severe gastritis and diffuse necrotic enteritis with antigen detection in the myenteric plexuses were observed in the suckling Syrian hamsters. This might be attributed to a high susceptibility of suckling Syrian hamsters to EHV-9 compared with adult ICR mice. The observed necrotic enteritis was similar to that described in infection with ADV (Zhao *et al.*, 1996). Following oral inoculation of other neurotropic viruses (e.g. herpes simplex virus), the myenteric and Meisner's

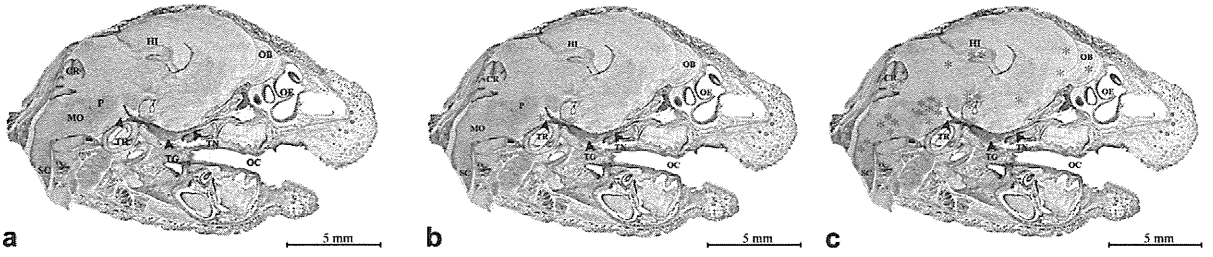

Fig. 12. Distribution of EHV-9 antigen in the brain of suckling hamsters (a) at 12 hpi, (b) at 48 hpi and (c) at 96 hpi. *Presence of viral antigen; OC, oral cavity; OE, olfactory epithelium; TN, trigeminal nerve; TG, trigeminal ganglia; TR, trigeminal root; OB, olfactory bulb; HI, hippocampus; CR, cerebellum; P, pons; MO, medulla oblongata; SC, spinal cord. IHC. Bar, 5 mm.

plexuses played essential roles in transmitting the virus to the CNS (Ha-Lee *et al.*, 1995; Gesser and Koo, 1996).

In the liver, foci of degenerative and necrotic hepatocytes, as well as the formation of intranuclear inclusions, were detected in the hepatocytes in both ICR mice and suckling hamsters. Moreover, positive EHV-9 immunolabelling implied virus replication, suggesting that the liver was a possible target organ for EHV-9 infection. Similar results were obtained after intraperitoneal inoculation of EHV-9 in suckling hamsters (El-Nahass *et al.*, 2011). A number of previous studies of EHV-1 infection have shown that the liver plays an important role in virus replication, especially during the initial stages of infection (Plummer *et al.*, 1973).

In conclusion, after oral inoculation of EHV-9 and based on time–course histopathological and immunohistochemical findings, it can be concluded that EHV-9 replicated and propagated in macrophages, especially in those in the submucosa of the oral cavity and tongue, and that these infected macrophages then spread to the maxillary and mandibular branches of the trigeminal nerve, followed by infection in the trigeminal ganglia and, finally, the CNS.

Acknowledgments

This study was supported in part by a grant-in-aid (emerging–general) for scientific research from the Ministry of Health, Labor and Welfare of Japan and a grant from the Ono Pharmaceutical Co, Ltd. We thank Miss C. Swift for proofreading the manuscript.

Conflict of Interest

The authors declare that they have no conflicts of interest with respect to their authorship or the publication of this article.

References

Aleman N, Quiroga MI, Lopez-Pena M, Vazquez S, Guerrero FH *et al.* (2001) Induction and inhibition of apoptosis by pseudorabies virus in the trigeminal ganglion during acute infection of swine. *Journal of Virology*, **75**, 469–479.

Bonina L, Iannello D, Merendino R, Arena A, Mastroeni P (1983) Tumor-dependent resistance of rat peritoneal macrophages to herpes simplex virus. *Infection and Immunity*, **39**, 575–579.

Borchers K, Wolfinger U, Lawrenz B, Schellenbach A, Ludwig H (1997) Equine herpesvirus 4 DNA in trigeminal ganglia of naturally infected horses detected by direct in situ PCR. *Journal of General Virology*, **78**, 1109–1114.

Donovan TA, Schrenzel MD, Tucker T, Pessier AP, Bicknese B *et al.* (2009) Meningoencephalitis in a polar bear caused by equine herpesvirus 9 (EHV-9). *Veterinary Pathology*, **46**, 1138–1143.

Edington N, Bridges CG, Patel JR (1986) Endothelial cell infection and thrombosis in paralysis caused by equid herpesvirus 1: equine stroke. *Archives of Virology*, **90**, 111–124.

El-Habashi N, El-Nahass E, Fukushi H, Hibi D, Sakai H *et al.* (2010a) Experimental intranasal infection of equine herpesvirus 9 (EHV-9) in suckling hamsters: kinetics of viral transmission and inflammation in the nasal cavity and brain. *Journal of Neurovirology*, **16**, 1–7.

El-Habashi N, El-Nahass E, Namihira Y, Hagiwara H, Fukushi H *et al.* (2011) Neuropathogenicity of equine herpesvirus 9 in cattle. *Journal of Equine Veterinary Science*, **31**, 72–77.

El-Habashi N, Murakami M, El-Nahass E, Hibi D, Sakai H *et al.* (2010b) Study on infectivity of EHV 9 (EHV-9) by different routes of inoculation in hamsters. *Veterinary Pathology*, **47**, 1–7.

El-Nahass E, El-Habashi N, Nayel M, Kasem S, Fukushi H *et al.* (2011) Kinetics and pathogenicity of equine herpesvirus-9 infection following intraperitoneal inoculation in hamsters. *Journal of Comparative Pathology*, doi: 10.1016/j.jcpa.2011.01.009.

Fukushi H, Taniguchi A, Yasuda K, Yanai T, Masegi T *et al.* (2000) A hamster model of equine herpesvirus 9 induced encephalitis. *Journal of Neurovirology*, **6**, 314–319.

Fukushi H, Tomita T, Taniguchi A, Ochiai Y, Kirisawa R *et al.* (1997) Gazelle herpesvirus 1: a new neurotropic herpesvirus immunologically related to equine herpesvirus 1. *Virology*, **227**, 34–44.

Gesser RM, Koo SC (1996) Oral inoculation with herpes simplex virus type 1 infects enteric neurons and mucosal nerve fibers within gastrointestinal tract of mice. *Journal of Virology*, **70**, 4097–4102.

Hagemoser WA, Kluge JP, Hill HT (1980) Studies on the pathogenesis of pseudorabies in domestic cats following oral inoculation. *Canadian Journal of Comparative Medicine*, **44**, 192–202.

Ha-Lee YM, Dillon K, Kosaras B, Sidman R, Revell P *et al.* (1995) Mode of spread to and within the central nervous system after oral inoculation of neonatal mice with AD strain of Theiler's murine strain encephalitis virus. *Journal of Virology*, **69**, 7354–7361.

Hasebe R, Kimura T, Sato E, Okazaki K, Ochiai K *et al.* (2002) Equine herpesvirus-1 induced encephalomyelitis in mice: a comparative study of neuroadapted virus and its parental strain. *Journal of Comparative Pathology*, **127**, 118–125.

Kodama A, Yanai T, Yonemaru K, Sakai H, Masegi T *et al.* (2007) Acute neuropathogenicity with experimental infection of equine herpesvirus 9 in common marmosets (*Callithrix jacchus*). *Journal of Medical Primatology*, **36**, 335–342.

Kritas SK, Nauwynck HJ, Pensaert MB (1995) Dissemination of wild-type and gC-, gE- and gI-deleted mutants of Aujeszky's disease virus in the maxillary nerve and trigeminal ganglion of pigs after intranasal inoculation. *Journal of General Virology*, **76**, 2063–2066.

Laast VA, Pardo CA, Tarwater PM, Queen SE, Reinhart TA *et al.* (2007) Pathogenesis of simian immunodeficiency virus-induced alterations in macaque trigeminal ganglia. *Journal of Neuropathology and Experimental Neurology*, **66**, 26–34.

Moolenbeek C, Ruitenberg EJ (1981) The 'Swiss roll': a simple technique for histological studies of the rodent intestine. *Laboratory Animals*, **15**, 57–59.

Narita M, Uchimura A, Kimura K, Tanimura N, Yanai T *et al.* (2000) Brain lesions and transmission of experimental equine herpesvirus type 9 in pigs. *Veterinary Pathology*, **37**, 476–479.

Plummer G, Coleman P, Cleveland P, Henson D (1973) Neurovirulence of equine herpes type 1 in mice of different ages. *Journal of Infectious Diseases*, **128**, 202–210.

Pusterla N, Mapes S, Wilson WD (2010) Prevalence of equine herpesvirus type 1 in trigeminal ganglia and submandibular lymph nodes of equids examined postmortem. *Veterinary Record*, **67**, 376–379.

Roscic-Mrkic B, Schwender RA, Odermatt B, Zuniga A, Pavovic J *et al.* (2001) Roles of macrophages in measles virus infection of genetically modified mice. *Journal of Virology*, **75**, 3343–3351.

Sasseville VG, Lackner AA (1997) Neuropathogenesis of simian immunodeficiency virus infection in macaque monkeys. *Journal of Neurovirology*, **3**, 1–9.

Schrenzel MD, Tucker TA, Donovan TA, Martin DM, Busch MD *et al.* (2008) New hosts for equine herpesvirus 9. *Emerging Infectious Diseases*, **14**, 1616–1619.

Steiner I, Kennedy PG (1995) Herpes simplex virus latent infection in the nervous system. *Journal of Neurovirology*, **1**, 19–29.

Taniguchi A, Fukushi H, Matsumura T, Yanai T, Masegi T *et al.* (2000a) Pathogenicity of a new neurotropic equine herpesvirus 9 (gazelle herpesvirus 1) in horses. *Journal of Veterinary Medical Science*, **62**, 215–218.

Taniguchi A, Fukushi H, Yanai T, Masegi T, Hirai K (2000b) Equine herpesvirus 9-induced lethal encephalitis in experimentally infected goats. *Archives of Virology*, **145**, 2619–2627.

Villarreal D, Young CR, Storts R, Tinng JW, Welsh CJ (2006) A comparison of the neurotropism of Theiler's virus and poliovirus in CBA mice. *Microbial Pathogenesis*, **41**, 149–156.

Waki K, Freed EO (2010) Macrophages and cell–cell spread of HIV-1. *Viruses*, **2**, 1603–1620.

Wu L (2008) Biology of HIV mucosal transmission. *Current Opinion in HIV and AIDS*, **3**, 534–540.

Yanai T, Fujishima N, Fukushi H, Hirata A, Sakai H *et al.* (2003a) Experimental infection of equine herpesvirus 9 in dogs. *Veterinary Pathology*, **40**, 263–267.

Yanai T, Sakai T, Fukushi H, Hirai K, Narita M *et al.* (1998) Neuropathological study of gazelle herpesvirus 9 (equine herpesvirus 9) infection in Thomson's gazelles (*Gazella thomsoni*). *Journal of Comparative Pathology*, **119**, 159–168.

Yanai T, Tsujioka S, Sakai H, Fukushi H, Hirai K *et al.* (2003b) Experimental infection with equine herpesvirus 9 (EHV-9) in cats. *Journal of Comparative Pathology*, **128**, 113–118.

Zhao YM, Narita M, Kawashima K (1996) Pathologic changes in closed porcine intestinal loops inoculated with Aujeszky's disease virus. *Journal of Veterinary Medical Science*, **58**, 809–810.

Zink MC, Laast AV, Helke KL, Brice AK, Barber SA *et al.* (2006) From mice to macaques – animal models of HIV nervous system disease. *Current HIV Research*, **4**, 293–305.

[*Received, April 4th, 2011*
Accepted, May 13th, 2011]

Parasitol Res (2012) 111:1019–1024
DOI 10.1007/s00436-012-2926-6

ORIGINAL PAPER

The use of different diagnostic tools for *Babesia* and *Theileria* parasites in cattle in Menofia, Egypt

Mohamed Nayel · Khaled Mohamed El-Dakhly · Mahmoud Aboulaila · Ahmed Elsify · Hany Hassan · Elsayed Ibrahim · Akram Salama · Tokuma Yanai

Received: 17 March 2012 / Accepted: 10 April 2012 / Published online: 29 April 2012

Abstract Bovine piroplasmosis is caused by tick-borne hemoprotozoans of the genera *Babesia* and *Theileria* and is the most prevalent in tropical and subtropical countries, causing a major economic impact worldwide. In the current study, a total of 405 cattle of different ages, sexes, and breeds were randomly sampled for surveying and diagnosis of babesiosis and theileriosis using three methods: direct microscopy (blood smears), indirect fluorescent antibody test (IFAT) and polymerase chain reaction (PCR). Giemsa-stained blood smears revealed that, out of 405 examined cattle, 33 (8.15 %) were infected with *Babesia* sp. and 65 (16.05 %) with *Theileria* sp. (total number of infected cattle was 98). Mixed infection was seen in 11 (2.72 %) animals. Moreover, application of the three diagnostic assays on 158 randomly sampled cattle indicated that 17 (10.76 %) and 33 (20.89 %) were positive for *Babesia* and *Theileria* spp. by the direct smear technique, 25 (15.82 %) and 33 (20.89 %) by IFAT (fluorescence was greenish yellow for *Babesia* and yellowish for *Theileria*), and 20 (12.66 %) and 38 (24.05 %) by PCR. Using primers specific for *Babesia* and *Theileria* spp., we found that diagnostic bands appeared at ~350 and ~370 bp, respectively indicating the presence of these piroplasms. Statistically, there was a non-significant difference of the positivity in response to the three techniques; thus, any of these methods can be described as useful for diagnosing blood parasites in both domesticated animals and birds. On the basis of the obtained results, it could be concluded that direct microscopy can be used in acute infections, whereas IFAT and PCR are useful in chronicity.

M. Nayel · A. Elsify · H. Hassan · A. Salama
Department of Animal Medicine and Infectious Diseases,
Faculty of Veterinary Medicine, Menofia University,
Sadat City, Egypt

K. M. El-Dakhly
Department of Parasitology, Faculty of Veterinary Medicine,
Beni-Suef University,
Beni-Suef 62511, Egypt

M. Aboulaila
Department of Parasitology, Faculty of Veterinary Medicine,
Menofia University,
Sadat City, Egypt

E. Ibrahim
Department of Animal Medicine and Infectious Diseases,
Faculty of Veterinary Medicine, Benha University,
Benha, Egypt

K. M. El-Dakhly · T. Yanai (✉)
Department of Veterinary Pathology,
Faculty of Applied Biological Science, Gifu University,
1-1 Yanagido,
Gifu 501-1193, Japan
e-mail: yanai@gifu-u.ac.jp

Introduction

Babesia and *Theileria* species are apicomplexan–hemoprotozoan parasites transmitted by Ixodidae ticks (Preston 2001; Silva et al. 2010) and are viewed to be devastating parasites affecting the production of livestock, mainly cattle and small ruminants. They pose a significant problem for veterinary authorities, occasionally emerging in conjunction with other disease conditions, and thus being difficult to pinpoint (Altay et al. 2008). These infections are of worldwide importance and are characterized by anemia, icterus, hemoglobinuria, and death, and as a result, they have a high economic impact in several parts of the world, including tropical and temperate countries (Wagner et al. 2002).
Bovine babesiosis is caused by multiple species: *Babesia bigemina*, *Babesia divergens*, *Babesia bovis*, and *Babesia major*. *Babesia* species have the potential for wide

distribution wherever their tick vectors are encountered. Two species, *B. bigemina* and *B. bovis*, have a considerable impact on cattle health and productivity in tropical and subtropical countries. Cattle suffering from theileriosis demonstrate varying clinical signs that range from lymphoproliferative changes with high morbidity and mortality, as seen with *Theileria annulata* and *Theileria parva*, to benign or mild disease, as seen with *Theileria orientalis* (Altay et al. 2008; Safieldin et al. 2011).

Detection of these blood parasites is highly beneficial in early diagnosis. Traditionally, microscopy using Giemsa-stained blood smears has been considered the "gold standard" for detecting *Babesia* and *Theileria* organisms in the blood of infected animals, particularly in acute cases, but not in carriers, where the parasitemia is low, with small numbers of the protozoa in the peripheral blood (Friedhoff and Bose 1994; Bose et al. 1995). Therefore, serological techniques were proposed for detecting circulating antibodies against these parasites, particularly in subclinical infections during epidemiological investigations. In addition, serological diagnosis using the indirect fluorescent antibody test can be used to detect antibodies against the *Theileria* species (Leemans et al. 1997). One disadvantage of such tests is the occurrence of false-positive and false-negative results, involving cross-reactions or improper specific immune response (Passos et al. 1998), while another is the inability to differentiate between previous and current infections, making sensitive and highly specified diagnostic techniques for *Babesia* and *Theileria*. Therefore, the application of PCR-based techniques is imperative in order to detect these hemoparasites in carrier animals (Criado-Fornelio et al. 2009). These methods were used for diagnosis of babesiosis and theileriosis in several species of related countries, showing similar climatic conditions, including Tunisia (M'ghirbi et al. 2008), United Arab Emirates (Jaffar et al. 2010) and Iran (Zaeemi et al. 2011).

The present study was performed for the purpose of surveying and diagnosing both *Babesia* and *Theileria* spp. in cattle in Menofia province, Egypt, using Giemsa-stained blood films, indirect fluorescent antibody test (IFAT)-serological test, and PCR assay.

Materials and methods

Animals and the study area

A total of 405 cattle of different ages, sexes, and breeds were clinically examined for diagnosis of *Babesia* and *Theileria* spp. during field trips in Menofia province (coordinates: 30 °03′00″ N 31 °15′00″ E), Egypt. Animals suffered from signs of blood parasites that were typical indications of babesiosis and theileriosis. Blood smears and blood samples were collected to confirm clinical diagnosis of both diseased and carrier animals.

Blood smears

Thin smears were prepared from EDTA-whole blood on clean and dry slides, fixed in methanol, stained with Giemsa stain, and microscopically examined for the detection of intra-erythrocytic forms of both *Babesia* and *Theileria* spp. piroplasms at 100× objective magnification. The smears were recorded as negative for piroplasms if no parasites were detected in 50 oil-immersion fields (Moretti et al. 2010).

Blood samples

Blood samples were collected for both PCR (with anticoagulant, sodium salt of EDTA) and IFAT (without anticoagulant). Blood was collected from the jugular vein and immediately preserved in Eppendorf tubes containing a few drops of EDTA.

Laboratory assays

Indirect fluorescent antibody test

Available parasite-coated slides for both *Babesia* and *Theileria* antigens were kindly provided by the Veterinary Serum and Vaccine Research Institute, Abassia, Egypt, ready for the indirect fluorescent antibody test as described by Leeflang and Perie (1972). A positive reaction is indicated by a bright fluorescence (Papadopoulos et al. 1996).

Polymerase chain reaction

DNA extraction and amplification DNA extraction was performed according to the Manual Chemical Method (rapid isolation of mammalian DNA) using cell lysis buffer (pH 8.0), ethanol (70 %), isopropanol, potassium acetate solution, red blood cell lysis buffer, and proteinase K (20 mg/ml) as described by Sambrook and Russell (2001).

PCR amplification was performed in a final reaction volume of 50 μl containing 200 μM of each dNTPs, 0.2 uM of each primer, 2.5 U of Taq DNA polymerase (Fermentas, Germany), 10 mM of TBE (tris, boric acid, and EDTA) buffer pH 8.0 containing 1.5 mM $MgCl_2$ and 5 μl of the DNA template. The designated primers were obtained from Bioneer Corporation (064550), Korea. The oligonucleotide sequences of the primers used were forward strand primer BAB GF2 (5′-GTC TTG TAA TTG GAA TGA TGG-3′) and reverse strand primer BAB GR2 (5′-CCA AAG ACT TTG ATT TCT CTC-3′) (Adaszek and Winiarczyk 2008) under the following conditions: an initial denaturation at 95 °C for 5 min followed by 40 cycles of

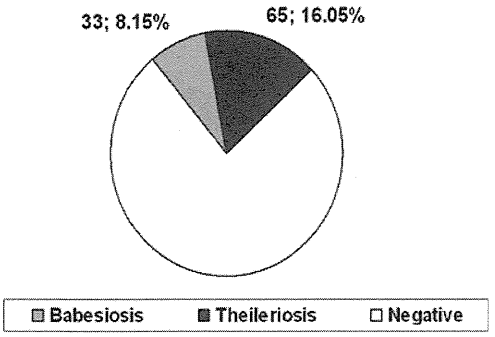

Fig. 1 Diagrammatic scale showing the overall prevalence of *Babesia* and *Theileria* parasites among the examined cattle in Menofia province

denaturation at 95 °C for 1 min, annealing at 55 °C for 1 min, and extension at 72 °C for 1 min, followed by final extension at 72 °C for 10 min.

The amplification reactions were carried out in a PCR thermal cycler Biometra T- personal/Germany S/N 1205334 and the corresponding amplicons were checked on 1.5 % agarose gel, stained with ethidium bromide, examined under UV transilluminator, and photographed using a digital camera.

Statistical analysis

Data were analyzed using multiple comparisons between different diagnostic methods for *Babesia* and *Theileria* parasites, including direct microscopy, IFAT, and PCR using the general linear model, Tukey test. This was carried out using Minitab statistical software (MTW13) (Raza et al. 2007). $P<0.05$ was accepted to be statistically significant.

Results

In this study, parasitological examination of 405 randomly selected cattle, by direct microscopy using Giemsa-stained thin blood films, revealed that 98 had intra-erythrocytic stages of piroplasms of both *Babesia* and *Theileria* spp. with an overall prevalence of 24.2 %. Among those, 33 (8.15 %) were infected by *Babesia* sp., 65 (16.05 %) had *Theileria* sp., and 11 cases showed mixed infection (Fig. 1). These results were consistent with the clinical signs and previous case histories taken from the farmers and owners of animals that were collected from different districts in Menofia province. As a result of chronic infection, the developing antibodies reacted positively using the IFAT, producing a fluorescence that was clearly distinct and greenish yellow (Fig. 2) or yellowish (Fig. 3) in color and indicated the presence of the intra-erythrocytic stages of both *Babesia* and *Theileria* piroplasms, respectively. PCR findings showed that diagnostic bands were produced at ~350 and ~370 bp, and the fragments were specific for both *Babesia* and *Theileria* spp., respectively (Fig. 4). This

Fig. 2 Greenish yellow fluorescence (*arrow*) indicating intra-erythrocytic stages of *Babesia* sp. piroplasms using IFAT (×100)

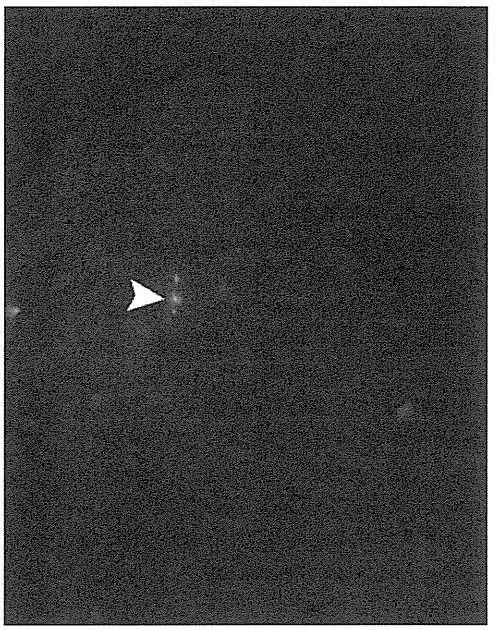

Fig. 3 Yellowish fluorescence of *Theileria* sp. piroplasms (*arrow*) indicating positive reaction with IFAT (×100)

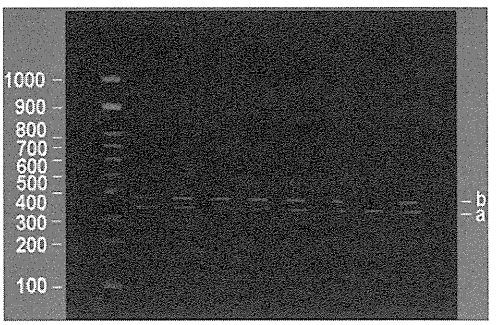

Fig. 4 PCR results showing diagnostic bands at 350-bp for *Babesia* (**a**) and 370bp for *Theileria* (**b**). *Lane M* 100-bp ladder=DNA marker (from Fermentas, Germany)

Table 1 Comparative detection of *Babesia* and *Theileria* parasites in cattle using direct microscopy, IFAT, and PCR

Parasite	Assay (n=158)						*P value*
	Direct microscopy		IFAT		PCR		
	Infected	Percent	Infected	Percent	Infected	Percent	
Babesia sp.	17	10.76	25	15.82	20	12.66	NS
Theileria sp.	33	20.89	33	20.89	38	25.05	NS

finding revealed the presence of both hemoparasites in the blood of examined cattle.

Furthermore, the seroprevalence of *Babesia* and *Theileria* species in cattle using IFAT revealed that out of 158 serum samples examined for the presence of antibodies, 25 (15.82 %) and 33 (20.89 %) were positive for *Babesia* spp. and *Theileria* spp., respectively. Furthermore, PCR findings indicated that 20 (12.66 %) and 38 (24.05 %) were positive for *Babesia* and *Theileria* spp., respectively (Table 1).

The findings in the present study confirmed that the use of direct microscopy, IFAT, or PCR is valuable in the diagnosis of *Babesia* and *Theileria* spp. Based on the confidence intervals calculated using the Tukey method (Minitab), it has been found that the differences between the three methods were not statistically significant, as there was no pairwise variation between infected animals (Fig. 5). This means that in some instances, mainly acute infections, the use of any of these methods may be applicable, although IFAT and PCR are preferable in chronic infections. It is worth mentioning that the methodology in the present investigation is based on collecting a considerable number of animals regardless of studying the effects of sex, age, or season on the infection level.

Discussion

Babesiosis and theileriosis have extensive prevalence and mortality rates with high economic losses in several countries (Shahnawaz et al. 2011). In Egypt, large numbers of cattle are infected with subclinical piroplasmosis (Adham et al. 2009). In such cases, in addition to the parasitological examination of stained blood films for detecting the *Babesia* protozoan parasites, low parasitemia necessitates the use of more advanced diagnostic tools, rather than conventional ones, to detect specific antibodies. In addition, negative microscopic examination does not exclude the possibility of infection (Weiland and Reiter 1988). Subclinical babesiosis and theileriosis lead to the affected livestock, including cattle and small ruminants, becoming chronic carriers of the piroplasms and in turn sources of infection for tick vectors, and cause natural transmission of the disease. Therefore, latent infections are the target in the epidemiology of the diseases.

In the present study, the results obtained from Giemsa-stained blood smears revealed that 33 smears (8.1 %) were positive for *Babesia*. Similar results were obtained by Sevnc et al. (2001) in Turkey and Mazyad and Khalaf (2002) in Egypt. On the other hand, Jeon (1978) in Korea and Osaki et al. (2002) in Brazil detected infection rates of 23 and 64 %, respectively. Fluctuation in the prevalence rates might be due to the variation of environmental conditions that affect both parasites and vectors. For *Theileria* sp., the present investigation showed that 65 (16.05 %) of 405 cattle were positive. These results agreed with those obtained by Jeon (1978) in Korea (17 %), Acici (1995) in Turkey (17 %), and those obtained in Egypt, which included Abu El-Magd (1980) in Quena province (11.1 %) and Adel (2007) in Gharbia province (11.31 %). Conversely, our results opposed a number of reports in Egypt, among them El Bahy (1986), who revealed prevalence rates of 65 and 53 % in cattle and buffaloes, respectively, and Gamal EI-Dien (1993) in El-Behera province, who found that the prevalence of *T. annulata* was 65.4 % using stained blood films.

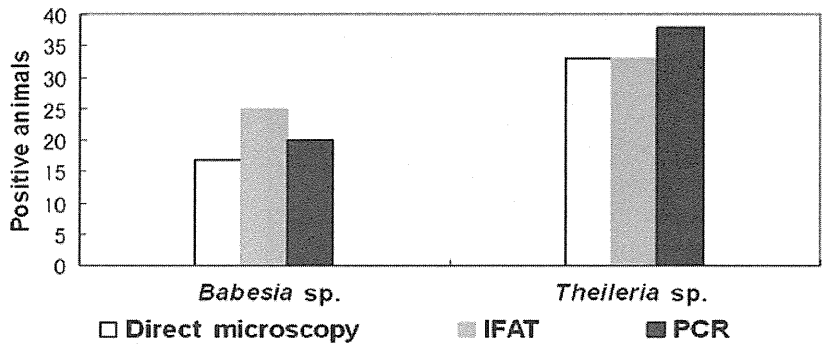

Fig. 5 Comparison of the positivity of *Babesia* and *Theileria* spp. using three diagnostic techniques: direct microscopy, IFAT, and PCR

Variation in prevalence rates could possibly be attributed to an abundance of the vectors as a result of high temperature and humidity. The present investigation showed that mixed infection, using Giemsa-stained blood smears, of *Babesia* and *Theileria* spp. appeared in 11 (2.72 %) of 405 examined cattle. These results coincided with those obtained by Dumanli and Ozer (1987) in Turkey, who found a mixed infection rate for *B. bigemina* and *T. annulata* of 1.5 % in cattle.

Using IFAT, the present study revealed an infection rate of 15.82 % (25/158) for *Babesia* sp. This finding was in accordance with that obtained by Terkawi et al. (2012), who examined a herd of cattle in the central region of Syria using IFAT and found infection rates of 18.36 and 21.74 % for *B. bovis* and *B. bigemina*, respectively. Moreover, Jaffar et al. (2010) in Dubai, UAE recorded infection rates of 10.5 and 33.3 % for equine babesiosis and theileriosis. On the other hand, Singh et al. (2009) recorded a rate of 56.11 % for *B. bigemina* in India, Iseki et al. (2010) noted rates of 68.8 and 75.8 % for *B. bovis* and *B. bigemina* in Thailand, and Sevgili et al. (2010) recorded an infection rate of 43.9 % for *B. bigemina* in Sanliura, Turkey. The variation in infection rates could be due to differences in climatic conditions and species of cattle. Concerning *Theileria* sp., the current investigation revealed that out of 158 bovine serum samples, 33 (20.89 %) was found to be positive for *Theileria* antibodies. This result agreed with that obtained by Sayin et al. (2003), who noted that 34 (21 %) of 155 examined cattle were found to be seropositive for *T. annulata*. Moreover, Adel (2007) in Gharbia province, Egypt reported that the incidence peaks of *T. annulata* seropositive native breed cattle using IFAT were 27.8 and 22 % in spring and summer, respectively. On the other hand, Gamal EI-Dien (1993) in EI-Behera province, Egypt detected that the prevalence of *T. annulata* was 71.9 %, and Caille (1987) in Somalia found that 71.2 % of cattle had antibodies against *T. annulata*. This discrepancy may be due to variation in the susceptibility of the animal species and could also be due to variance in animal locale.

Results of PCR revealed that 20 (12.66 %) of 158 animals were positive for *Babesia* sp. These findings were similar to those mentioned by Oliveira-Sequeira et al. (2005), who recorded a 10 % infection rate for *Babesia* using PCR and M'ghirbi et al. (2008) who revealed an infection rate of 11.11 % for bovine *Babesia* spp. Similar results were obtained by Figueroa et al. (1993) and Gubbels et al. (2002). On the other hand, De Vos and Potgieter (1994) in France found a 20 % infection rate, Costa-Junior et al. (2006) in Brazil found that 8 of 30 cattle (26.7 %) were positive for *Babesia* infection using PCR, and Rania (2009) in Egypt mentioned that the infection rate of *Babesia* sp. was 25.33 %. These discrepancies could be due to changes in locale. The infection rate of *Theileria* using PCR indicated that 60 animals (21.8 %) were positive. This result was similar to those cited by Ogden et al. (2003), Aktas et al. (2005), Altay et al. (2007) and M'ghirbi et al. (2008). Ogden et al. found an infection rate of 23.4 % for *Theileria* sp. in cows in Tanzania using PCR.

The authors concluded that the three techniques, direct microscopy, IFAT, and PCR, are all methods of choice with slight variation in their results, and this was confirmed by obtaining non-significant findings among them. Consequently, they are used in the detection of prevalence of blood parasites, primarily *Babesia* and *Theileria*. Direct microscopy with Giemsa-stained blood films is the conventional and the more practical method on farms, as it is rapid and inexpensive, but it is useful only in acute infections. Moreover, IFAT and PCR are modern assays that help veterinarians detect protozoan parasites in chronic carrier animals, and they circumvent the problem of false negative results obtained under direct microscopy.

Acknowledgments The authors are grateful to veterinarians and farmers in Menofia province, Egypt, who provided assistance in collecting samples. We also offer our sincere thanks to Dr. El-Shyamaa Nabil for providing statistical guidance in the study.

References

Abu El-Magd MM (1980) Some epidemiological studies about theileriosis at Quna Governorate. PhD. thesis, Faculty of Veterinary Medicine, Assuit University, Assuit, Egypt

Acici M (1995) Prevalence of blood parasites in cattle in the Samsun region, Turkey. Etlik Vet Mikrob Derg 8:271–277

Adaszek L, Winiarczyk S (2008) Molecular characterization of *Babesia canis canis* isolates from naturally infected dogs in Poland. Vet Parasitol 152:235–241

Adel EM (2007) Studies on some blood parasites infecting farm animals in Gharbia
governorate, Egypt. PhD thesis, Faculty of Veterinary Medicine, Cairo University, Cairo, Egypt

Adham FK, Abd-El-Samie EM, Gabre RM, El Hussein H (2009) Detection of tick blood parasites in Egypt using PCR assay I—*Babesia bovis* and *Babesia bigemina*. Parasitol Res 105:721–730

Aktas M, Altay K, Dumanli N (2005) Development of a polymerase chain reaction method for diagnosis of *Babesia ovis* infection in sheep and goats. Vet Parasitol 133:277–281

Altay K, Dumanli N, Aktas M (2007) Molecular identification, genetic diversity and distribution of *Theileria* and *Babesia* species infecting small ruminants. Vet Parasitol 147:161–165

Altay K, Fatih Aydin M, Dumanli N, Aktas M (2008) Molecular detection of *Theileria* and *Babesia* infections in cattle. Vet Parasitol 158:295–301

Bose R, Jorgensen WK, Dalgliesh RJ, Friedhoff KT, De Vos AJ (1995) Current state and future trends in the diagnosis of babesiosis. Vet Parasitol 57:61–74

Caille JY (1987) Serological survey of the prevalence and seasonal incidence of haemoprotozoa in livestock in Somalia. Thesis, Freie Universitat Berlin, Berlin, Germany

Costa-Junior LM, Rabelo EML, Filho OAM, Ribeiro MFB (2006) Comparison of different direct diagnostic methods to identify *Babesia bovis* and *Babesia bigemina* in animals vaccinated with live attenuated parasites. Vet Parasitol 139:231–236

Criado-Fornelio A, Buling A, Pingret JL, Etievant M, Boucraut-Baralon C, Alongi A, Agnone A, Torina A (2009) Hemoprotozoa of domestic animals in France: prevalence and molecular characterization. Vet Parasitol 159:73–76

De Vos AJ, Potgieter FT (1994) Bovine babesiosis. In: Coetzer JAW, Thomson GR, Tustin RC (eds) Infectious diseases of livestock. Oxford University Press, Cape Town, pp 278–294

Dumanli N, Ozer E (1987) Elaziğ yöresinde sigirlarda görülen kan parazitleri ve yayihs¸jan üzerinde araştirmalar. Selcuk Ü nin. Vet Fak Derg 3:159–166

El Bahy NMA (1986) Some studies on ticks and tick borne disease among ruminants in Fayom Governorate. M.V.Sc. thesis (Parasitology), Faculty of Veterinary Medicine, Cairo University, Cairo, Egypt

Figueroa JV, Chieves LP, Johnson GS, Buening GM (1993) Multiplex polymerase chain reaction based assay for the detection of *Babesia bigemina*, *Babesia* bovis and *Anaplasma marginale* DNA in bovine blood. Vet Parasitol 50:69–81

Friedhoff K, Bose R (1994) Recent developments in diagnostics of some tick-borne diseases. In: Uilenberg, G., Permin, A., Hansen, J.W. (eds). Use of applicable biotechnological methods for diagnosing haemoparasites. Proceedings of the Expert Consultation, Merida, Mexico, October 4–6, 1993. Food and Agriculture Organization of the United Nations (FAO), Rome, Italy, pp 46–57

Gamal EI-Dien HY (1993) Studies on *Theileria* protozoan among cattle in Behera Province. M.V.Sc. thesis, Faculty of Veterinary Medicine, Alexandria University, Alexandria, Egypt

Gubbels MJ, Yin H, Bai Q, Liu G, Nijman IJ, Jongejan F (2002) The phylogenetic position of the *Theileria buffeli* group in relation to other *Theileria* species. Parasitol Res 88:S28–S32

Iseki H, Zhou L, Kim C, Inpankaew T, Sununta C, Yokoyama N, Xuan X, Jittapalapong S, Igarashi I (2010) Seroprevalence of *Babesia* infections of dairy cows in northern Thailand. Vet Parasitol 170:193–196

Jaffar O, Abdishakur F, Hakimuddin F, Riya A, Wernery U, Schuster RK (2010) A comparative study of serological tests and PCR for the diagnosis of equine piroplasmosis. Parasitol Res 106:709–713

Jeon Y (1978) A survey of babesiosis and theileriosis in Korean cattle. Korean J Vet Res 18:23–26

Leeflang MJ, Perie CD (1972) Duration of serological response to the indirect fluorescent antibody test of cattle recovered from *Theileria parva* infection. Res Vet Sci 14:270–271

Leemans I, Hooshmand-Rad P, Uggla A (1997) The indirect fluorescent antibody test based on schizont antigen for study of the sheep parasite *Theileria lestoquardi*. Vet Parasitol 69:9–18

M'ghirbi Y, Hurtado A, Brandika J, Khlif K, Ketata Z, Bouattour A (2008) A molecular survey of *Theileria* and *Babesia* parasites in cattle, with a note on the distribution of ticks in Tunisia. Parasitol Res 103:435–442

Mazyad SA, Khalaf SA (2002) Studies on Theileria and Babesia infecting live and slaughtered animals in Al Arish and El Hasanah, North Sinai Governorate, Egypt. J Egypt Soc Parasitol 32 (2):601–610

Moretti A, Mangili V, Salvatori R, Maresca C, Scoccia E, Torina A, Moretta I, Gabrielli S, Tampieri MP, Pietrobelli M (2010) Prevalence and diagnosis of *Babesia* and *Theileria* infections in horses in Italy: a preliminary study. Vet J 184:346–350

Ogden NH, Gwakisa P, Swai E, French NP, Fitzpatrick J, Kambarage D, Bryant M (2003) Evaluation of PCR to detect *Theileria parva* in field-collected tick and bovine samples in Tanzania. Vet Parasitol 112(3):177–183

Oliveira-Sequeira TC, Oliveira MC, Araujo JP Jr, Amarante AF (2005) PCR-based detection of *Babesia* bovis and *Babesia bigemina* in their natural host *Boophilus microplus* and cattle. Int J Parasitol 35:105–111

Osaki SC, Vidotto O, Marana ERM, Vidotto MC, Yoshihara E, Pacheco RC, Igarashi M, Minho AP (2002) Occurrence of antibodies against *Babesia bovis* and studies on natural infection in Nelore cattle, in Umuarama municipality, Paraná State, Brazil. Rev Bras Parasitol Vet 11:73–83

Papadopoulos B, Marie Perie N, Uilenberg G (1996) Piroplasms of domestic animals in the Macedonia region of Greece. 1. Serological cross-reactions. Vet Parasitol 63:41–56

Passos LM, Bell-Sakyi L, Brown CG (1998) Immunochemical characterization of in vitro culture-derived antigens of *Babesia bovis* and *Babesia bigemina*. Vet Parasitol 76:239–249

Preston PM (2001) Theilerioses. In: Wallingford MW (ed) Encyclopedia of arthropod-transmitted infections of man and domesticated animals. CABI, Wallingford, pp 487–502

Rania YE (2009) Some studies on diagnosis on babesiosis. M.V.Sc. thesis, Faculty of Veterinary Medicine, Benha University, Benha, Egypt

Raza MA, Iqbal Z, Jabbar A, Yaseen M (2007) Point prevalence of gastrointestinal helminthiasis in ruminants in southern Punjab, Pakistan. J Helminthol 81:323–328

Safieldin M, Abdel Gadir A, Elmalik Kh (2011) Factors affecting seasonal prevalence of blood parasites in dairy cattle in Omdurman locality, Sudan. J Cell Anim Biol 5(1):17–19

Sambrook J, Russell DW (2001) Molecular cloning: a laboratory manual, 3rd edn. Cold Spring Harbor Laboratory Press, New York

Sayin F, Dincer S, Karaer Z, Cakmak A, Inci A, Yukari BA, Vatansever Z, Nalbantoglu S (2003) Studies on the epidemiology of tropical theileriosis (*Theileria annulata* infection) in cattle in central Anatolia, Turkey. Trop Anim Health Prod 35(6):521–539

Sevgili M, Cakmak A, Gokcen A, Altas MG, Ergun G (2010) Prevalence of *Theileria annulata* and *Babesia bigemina* in cattle in the vicinity of Sanliurfa. J Anim Vet Adv 9(2):292–296

Sevnc F, Sevnc M, Brdane FM, Altnoz F (2001) Prevalence of *Babesia bigemina* in cattle. Rev Med Vet 152(5):395–398

Shahnawaz S, Ali M, Aslam MA, Fatima R, Chaudhry ZI, Hassan MU, Ali M, Iqbal F (2011) A study on the prevalence of a tick-transmitted pathogen, *Theileria annulata*, the hematological profile of cattle from Southern Punjab (Pakistan). Parasitol Res 109:1155–1160

Silva MG, Marques PX, Oliva A (2010) Detection of *Babesia* and *Theileria* species infection in cattle from Portugal using a reverse line blotting method. Vet Parasitol 174:199–205

Singh H, Mishra AK, Rao JR, Tewari AK (2009) Comparison of indirect fluorescent antibody test (IFAT) and slide enzyme linked immunosorbent assay (SELISA) for diagnosis of *Babesia bigemina* infection in bovines. Trop Anim Health Prod 41:153–159

Terkawi MA, Alhasan H, Huyen NX, Sabagh A, Awier K, Cao S, Goo Y, Aboge G, Yokoyama N, Nihikawa Y, Kalb-Allouz A, Tabbaa D, Igarashi I (2012) Molecular and serological prevalence of *Babesia bovis* and *Babesia bigemina* in cattle from central region of Syria. Vet Parasitol. doi:10.1016/j.vetpar.2011.12.038

Wagner GG, Holman P, Waghela S (2002) Babesiosis and heartwater: threats without boundaries. Vet Clin Food Anim 18:417–430

Weiland G, Reiter I (1988) Methods for measurement of the serological response to Babesia. In: Ristic M (ed) Babesiosis of domestic animals and man. CRC, Boca Raton, pp 143–162

Zaeemi M, Haddadzadeh H, Khazraiinia P, Kazemi B, Bandehpour M (2011) Identification of different *Theileria* species (*Theileria lestoquardi*, *Theileria ovis*, and *Theileria annulata*) in naturally infected sheep using nested PCR–RELP. Parasitol Res 108:837–843

J. Comp. Path. 2013, Vol. 148, 43–46

Available online at www.sciencedirect.com

SciVerse ScienceDirect

ELSEVIER

www.elsevier.com/locate/jcpa

DISEASE IN WILDLIFE OR EXOTIC SPECIES

Spontaneous T/NK-cell Lymphoma associated with Simian Lymphocryptovirus in a Japanese Macaque (*Macaca fuscata*)

A. Hirata*, Y. Tachikawa†, K. Hashimoto†, H. Sakai†, A. Kaneko‡, J. Suzuki‡, K. Eguchi§, K. Shigematsu¶, H. Nikami* and T. Yanai†

** Division of Animal Experiment, Life Science Research Center, † Laboratory of Veterinary Pathology, Department of Veterinary Medicine, Faculty of Applied Biological Sciences, Gifu University, Yanagido 1-1, Gifu 501-1194 and 501-1193, ‡ Center for Human Evolution Modelling Research, Primate Research Institute, Kyoto University, Kanbayashi, Inuyama, Aichi 484-8506, § Department of Biological Sciences, Graduate School of Science and Engineering, Tokyo Metropolitan University, 1-1 Minami-Osawa, Hachioji-shi, Tokyo, 192-0397 and ¶ Department of Pathology, Japanese Red Cross Nagasaki Genbaku Hospital, 3-15 Mori-machi, Nagasaki 852-8511, Japan*

Summary

A 5-year-old female Japanese macaque (*Macaca fuscata*) was humanely destroyed because of severe anaemia with poor response to treatment. At necropsy examination, marked splenomegaly and systemic enlargement of lymph nodes were observed. Microscopical examination revealed diffuse proliferation of neoplastic lymphoid cells in the spleen and lymph nodes with infiltration of the liver, lung, gastrointestinal tract, kidney and bone marrow. Immunohistochemically, the neoplastic cells expressed CD3 and CD4, but not CD20, CD79α or CD8, consistent with a T helper phenotype. A portion of neoplastic cells expressed the natural killer (NK) cell marker CD56. In-situ hybridization detected Epstein-Barr virus (EBV)-encoded small RNAs in the neoplastic cells, indicating the involvement of simian lymphocryptovirus (LCV). This is the first report of simian LCV-associated T/NK-cell lymphoma with the predominant expression of T-cell antigens in non-human primates.

Keywords: Japanese macaque; lymphocryptovirus; T/NK-cell lymphoma

Lymphomas are common, spontaneously arising tumours in non-human primates (Beniashvili, 1989). Certain viruses are associated with the development of lymphoma in non-human primates as well as in man. These include simian lymphocryptovirus (LCV) and simian T-cell lymphotropic virus (STLV). These viruses are closely related to Epstein-Barr virus (EBV) and human T-cell lymphotropic virus type I (HTLV-I), respectively. A significant percentage of Japanese macaques (*Macaca fuscata*) are seropositive for simian LCV (Ishida *et al.*, 1993) and STLV (Hayami *et al.*, 1984); however, there are only a few reports of lymphomas in Japanese macaques and it remains unclear whether those viruses are associated with the development of lymphoma.

A female Japanese macaque was born and reared at the Primate Research Institute of Kyoto University and had been kept in an outdoor group. At 5 years of age, the macaque suddenly exhibited an unsteady gait and a swelling of the left cheek that was due to a large abscess of the upper gingiva. Severe anaemia (red blood cell count 0.8×10^{12}/l, haemoglobin 2.0 g/dl and haematocrit 6.6%; normal reference intervals $4.5–6.0 \times 10^{12}$/l, 12–15 g/dl and 40–45%, respectively) and low platelet count (124×10^{9}/l; reference interval $200–300 \times 10^{9}$/l) were detected by means of haematological testing. The white blood cell count was not elevated (8.2×10^{9}/l; reference interval $7.0–12.0 \times 10^{9}$/l). Increases in alanine

Correspondence to: T.Yanai (e-mail: yanai@gifu-u.ac.jp).

0021-9975/$ - see front matter
doi:10.1016/j.jcpa.2012.05.001

aminotransferase (69 IU/l; reference interval 15—45 IU/l), blood urea nitrogen (11.4 mmol/l; reference interval 3.6—8.9 mmol/l) and C-reactive protein (1.3 mg/dl; reference interval <0.3 mg/dl) were detected by means of serum biochemistry. This macaque had not been examined serologically for simian LCV infection. After 5 days of treatment, the animal was humanely destroyed because of a poor prognosis and necropsy examination was performed immediately.

There was marked diffuse splenomegaly (the spleen measured 7 × 13 cm in length and width, respectively; normal size of spleen is 2—3 × 4—5 cm in length and width, respectively, in age-matched Japanese macaques) and enlargement of superficial and visceral lymph nodes (2.2 cm maximum dimension; normal lymph nodes are approximately 0.5 cm maximum dimension). The spleen was uniformly red in colour and the lymph nodes were cream in colour with loss of corticomedullary differentiation on cut surface.

Samples of the major organs and enlarged lymph nodes and a sample of sternal bone marrow were fixed in 10% neutral buffered formalin and processed routinely. Sections were stained with haematoxylin and eosin (HE). Microscopically, there was a diffuse proliferation of neoplastic lymphoid cells in the white pulp, cords and red pulp sinuses of the spleen (Fig. 1A). In the lymph nodes, the same neoplastic cells replaced the normal architecture and invaded the surrounding adipose tissues. Extensive necrosis was observed in some lymph nodes. Bone marrow infiltration was found and was thought likely to be the cause of the severe anaemia. In the liver, there was periportal and sinusoidal infiltration of neoplastic cells. Neoplastic cells were also observed in the lamina propria of the gastrointestinal tract and the interstitium of the kidneys. In addition, circulating neoplastic cells were frequently found in the blood vessels of various organs. In the lung, there were numerous neoplastic cells in the alveolar capillaries. The neoplastic infiltrates were composed of two types of mononuclear cell (Fig. 1B). The predominant population was of small, mature cells with hyperchromatic, round or oval nuclei and scant cytoplasm. These cells were similar to normal lymphocytes, but often contained irregular nuclei. Larger neoplastic cells were also observed. These had medium to large nuclei with a distinct, large nucleolus and a moderate amount of pale, eosinophilic cytoplasm.

Serial sections were subjected to immunohistochemistry (IHC) using polyclonal antibody specific for human CD3 (Dako, Glostrup, Denmark) and monoclonal antibodies specific for human CD4 (clone 1F6; Nichirei Biosciences Inc., Tokyo, Japan), CD8 (clone C8/144B; Nichirei Biosciences Inc.), CD20 (clone L26; Dako), CD56 (clone 1B6; Nichirei Biosciences Inc.), CD79α (clone HM57; Dako) and mouse Ki-67 antigen (clone TEC-3; Dako). For 'visualization' of immunoreactivity, the EnVision System (Dako) was used in conjunction with 3-amino-9-ethylcarbazole (ACE) or 3, 3′-diaminobenzidine (DAB) and sections were counterstained with haematoxylin.

The majority of the neoplastic cells, irrespective of the cell type, were positive for CD3 (Fig. 1C) and CD4, but negative for CD20, CD79α and CD8, exhibiting the T helper cell phenotype. The larger neoplastic cells were also positive for the natural killer (NK) cell marker CD56 (Fig. 1D). Both cell types expressed the proliferation marker Ki-67 (Fig. 1E).

To confirm the presence of simian LCV in neoplastic cells, in-situ hybridization (ISH) was performed on formalin-fixed and paraffin wax-embedded sections using peptide nucleic acid (PNA) probes complementary to EBV-encoded small RNAs (EBERs) (Epstein-Barr Virus PNA Probe, Dako). Signals for EBERs were 'visualized' using the PNA ISH detection Kit (Dako) and sections were counterstained with nuclear fast red. EBER transcripts were detected more frequently in the larger neoplastic cells than in the smaller neoplastic cells. The EBER-positive cells were scattered throughout the tumour tissues (Fig. 1F).

Like many other species of non-human primates, Japanese macaques are latently infected with the EBV-related herpesvirus, simian LCV (Carville and Mansfield, 2008). Previous studies have demonstrated that almost all Japanese macaques are seropositive for simian LCV (Ishida and Yamamoto, 1987; Ishida *et al.*, 1993). However, simian LCV infection is almost always subclinical and there is little evidence for the oncogenic potential of simian LCV in Japanese macaques. In the present case, ISH revealed EBER transcripts in the neoplastic lymphoid cells, indicating the role of simian LCV in the development of lymphoma. At present, it is impossible to detect EBER transcripts with specific probes for Japanese macaque LCV due to the lack of available sequence data, but we were able to detect the viral RNA with a probe used for the detection of EBV. Previous studies have shown that EBER genes are relatively conserved between EBV and simian LCVs (73 and 42% nucleotide identities between EBV and Rhesus macaque LCV in the EBER1 and EBER2 genes, respectively) and contain highly conserved regions (Rao *et al.*, 2000). In addition, it is unlikely that the probes detected transcripts from EBV, rather than simian LCVs in the neoplastic cells, because EBV is not pathogenic

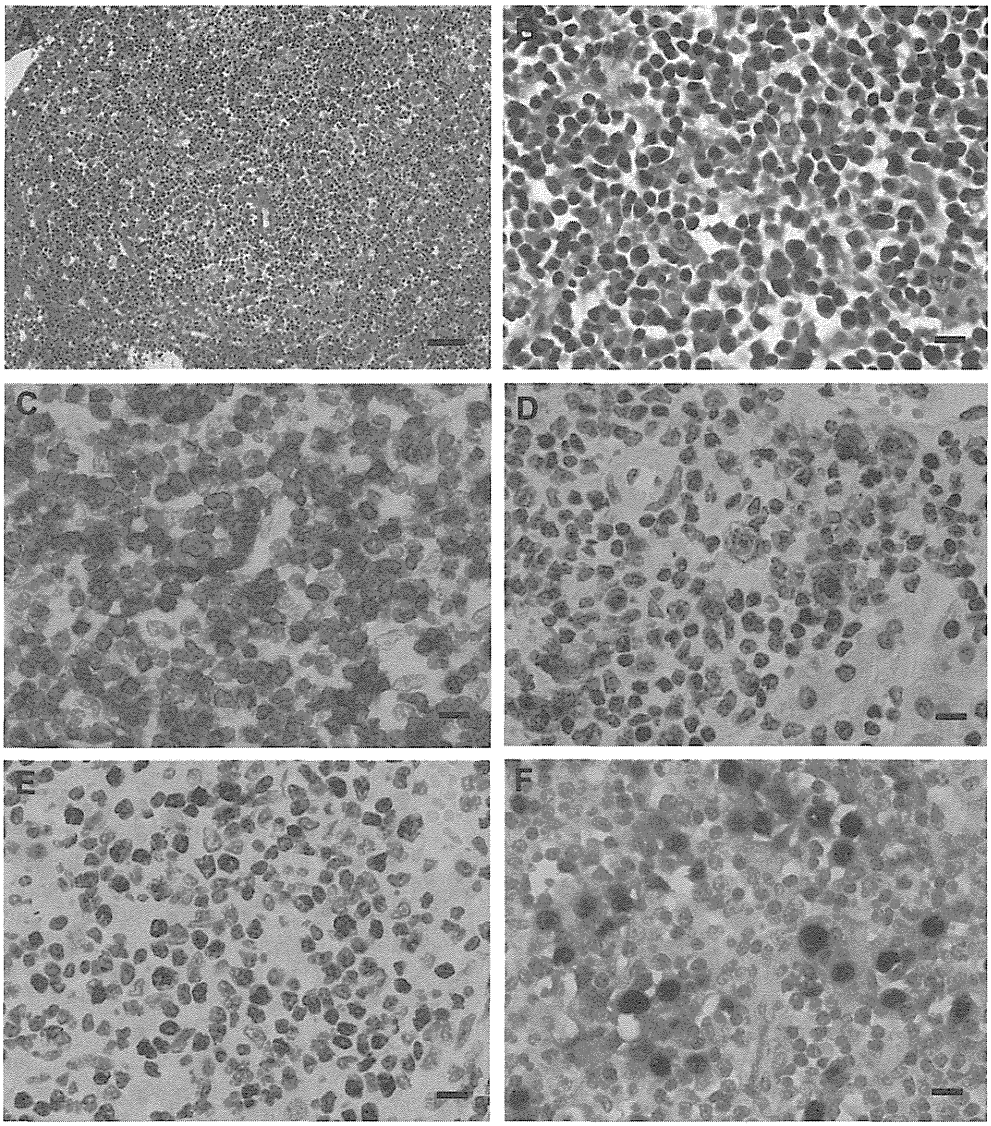

Fig. 1. Histopathology, IHC and ISH of the neoplastic lesions found in the spleen (A, B, C, D and F) and liver (E) of a Japanese macaque. (A) Neoplastic cells in the red and white pulp of the spleen. HE. Bar, 50 μm. (B) Higher magnification of (A). The lesions are composed of two types of neoplastic cells. HE. Bar, 10 μm. (C) The majority of the neoplastic cells express CD3. IHC. Bar, 10 μm. (D) The larger neoplastic cells show membrane expression of CD56. IHC. Bar, 10 μm. (E) Ki-67 is expressed by both types of neoplastic cells. IHC. Bar, 10 μm.(F) EBER transcripts are seen mainly in the larger neoplastic cells. ISH. Bar, 10 μm.

for macaques, as shown in experimental infection studies (Frank *et al.*, 1976; Levine *et al.*, 1980). Therefore, this diagnostic technique would facilitate the detection of simian LCV in histological sections of tissue from Japanese macaques and contribute to a better understanding of the pathogenicity of the virus.

In people, EBV has been implicated in the development of a wide range of B cell malignancies (Carbone *et al.*, 2008). Similarly, simian LCVs have been shown to be associated with B-cell lymphomas in non-human primates and this provides an important animal model for studying EBV-associated lymphoma (Feichtinger *et al.*, 1992; Pingel *et al.*, 1997; Carville and Mansfield, 2008). However, whereas EBV has been reported to be associated with several types of T/NK-cell lymphomas (Carbone *et al.*, 2008; Piccaluga *et al.*, 2011) it remains unclear whether simian LCVs also contribute to the development of these malignancies. Therefore, it is noteworthy that the present case clearly exhibited the immunophenotypes of T/NK cells that were positive for CD3 and CD56. To date, there has been only one report of T/NK-cell lymphoma associated with simian LCV. Interestingly, the previous case was also found in a Japanese macaque and was

diagnosed as the nasal type of NK/T-cell lymphoma based on the involvement of the nasal cavity, the absence of expression of the T-cell antigen CD3 and the predominant expression of the NK-cell antigen CD16 (Suzuki *et al.*, 2005). There was a distinct difference in CD3 expression between the present and previous cases and, therefore, this is the first report of simian LCV-associated T/NK-cell lymphoma with predominant expression of CD3 in non-human primates. It remains difficult to determine whether simian LCV preferentially induces T/NK-cell lymphoma in Japanese macaques. Further studies are needed to define the cell tropism of simian LCV in Japanese macaques, but the Japanese macaque may serve as a potential animal model of EBV-associated T/NK-cell lymphomas in man.

Acknowledgments

We thank Ms. C. Iriyama for expert technical assistance. This study was supported by the Cooperation Research Program of the Primate Research Institute of Kyoto University and a Grant-in-Aid for scientific research from the Ministry of Education, Culture, Sports, Science and Technology of Japan.

References

Beniashvili DS (1989) An overview of the world literature on spontaneous tumors in nonhuman primates. *Journal of Medical Primatology*, **18**, 423–437.

Carbone A, Gloghini A, Dotti G (2008) EBV-associated lymphoproliferative disorders: classification and treatment. *Oncologist*, **13**, 577–585.

Carville A, Mansfield KG (2008) Comparative pathobiology of macaque lymphocryptoviruses. *Comparative Medicine*, **58**, 57–67.

Feichtinger H, Li SL, Kaaya E, Putkonen P, Grunewald K *et al.* (1992) A monkey model for Epstein Barr virus-associated lymphomagenesis in human acquired immunodeficiency syndrome. *Journal of Experimental Medicine*, **176**, 281–286.

Frank A, Andiman WA, Miller G (1976) Epstein-Barr virus and nonhuman primates: natural and experimental infection. *Advances in Cancer Research*, **23**, 171–201.

Hayami M, Komuro A, Nozawa K, Shotake T, Ishikawa K *et al.* (1984) Prevalence of antibody to adult T-cell leukemia virus-associated antigens (ATLA) in Japanese monkeys and other non-human primates. *International Journal of Cancer*, **33**, 179–183.

Ishida T, Suzuki J, Yamamoto K (1993) Serological features of infection with an Epstein-Barr-virus-like agent in Japanese macaques (*Macaca fuscata*). *Folia Primatologica (Basel)*, **61**, 228–233.

Ishida T, Yamamoto K (1987) Survey of nonhuman primates for antibodies reactive with Epstein-Barr virus (EBV) antigens and susceptibility of their lymphocytes for immortalization with EBV. *Journal of Medical Primatology*, **16**, 359–371.

Levine PH, Leiseca SA, Hewetson JF, Traul KA, Andrese AP *et al.* (1980) Infection of rhesus monkeys and chimpanzees with Epstein-Barr virus. *Archives of Virology*, **66**, 341–351.

Piccaluga PP, Gazzola A, Agostinelli C, Bacci F, Sabattini E *et al.* (2011) Pathobiology of Epstein-Barr virus-driven peripheral T-cell lymphomas. *Seminars in Diagnostic Pathology*, **28**, 234–244.

Pingel S, Hannig H, Matz-Rensing K, Kaup FJ, Hunsmann G *et al.* (1997) Detection of Epstein-Barr virus small RNAs EBER1 and EBER2 in lymphomas of SIV-infected rhesus monkeys by in-situ hybridization. *International Journal of Cancer*, **72**, 160–165.

Rao P, Jiang H, Wang F (2000) Cloning of the rhesus lymphocryptovirus viral capsid antigen and Epstein-Barr virus-encoded small RNA homologues and use in diagnosis of acute and persistent infections. *Journal of Clinical Microbiology*, **38**, 3219–3225.

Suzuki J, Goto S, Kato A, Hashimoto C, Miwa N *et al.* (2005) Malignant NK/T-cell lymphoma associated with simian Epstein-Barr virus infection in a Japanese macaque (*Macaca fuscata*). *Experimental Animals*, **54**, 101–105.

[*Received, May 28th, 2011*
Accepted, May 2nd, 2012]